JOURNAL OF GEOPHYSICAL RESEARCH, VOL. 114, G04026, doi:10.1029/2008JG000919, 2009



# Modeling gross primary production of deciduous forest using remotely sensed radiation and ecosystem variables

Nasreen Jahan[1] and Thian Yew Gan[1]

Received 24 December 2008; revised 7 August 2009; accepted 21 September 2009; published 30 December 2009.

[1] We explored the potential application of two remotely sensed (RS) variables, the Global Vegetation Moisture Index (GVMI) and the near-infrared albedo ($Albedo_{NIR}$), in modeling the gross primary production (GPP) of three deciduous forests. For the Harvard Forest (deciduous) of Massachusetts, it was found that GPP is strongly correlated with GVMI (coefficient of determination, $R^2 = 0.60$) during the growing season, and with $Albedo_{NIR}$ ($R^2 = 0.82$) throughout the year. Subsequently, a statistical model called the Remotely Sensed GPP (R-GPP) model was developed to estimate GPP using remotely sensed radiation (land surface temperature (LST), $Albedo_{NIR}$) and ecosystem variables (enhanced vegetation index (EVI) and GVMI). The R-GPP model, calibrated and validated against the GPP estimates derived from the eddy covariance flux tower of the Harvard Forest, could explain 95% and 92% of the observed GPP variability for the study site during the calibration (2000–2003) and the validation (2004–2005) periods, respectively. It outperformed the primary RS-based GPP algorithm of Moderate Resolution Imaging Spectroradiometer (MODIS), which explained 80% and 77% of the GPP variability during 2000–2003 and 2004–2005, respectively. The calibrated R-GPP model also explained 93% and 94% of the observed GPP variation for two other independent validation sites, the Morgan Monroe State Forest and the University of Michigan Biological Station, respectively, which demonstrates its transferability to other deciduous ecoregions of northeastern United States.

**Citation:** Jahan, N., and T. Y. Gan (2009), Modeling gross primary production of deciduous forest using remotely sensed radiation and ecosystem variables, *J. Geophys. Res.*, *114*, G04026, doi:10.1029/2008JG000919.

## 1. Introduction

[2] The gross primary production (GPP) of an ecosystem represents the gross uptake of carbon dioxide ($CO_2$) by vegetation for photosynthesis. It is the primary conduit of carbon flux from atmosphere to land and a key source of energy that fuels economies. On the other hand, $CO_2$ from fossil fuel burning and ecosystem respiration is a major contributor to global warming or greenhouse effect. Fossil fuel burning has perturbed the carbon cycle, and affected the global climate, leading to worldwide research on climate change and the carbon cycle [*Intergovernmental Panel on Climate Change*, 2007; *Heinsch et al.*, 2006; *Urbanski et al.*, 2007]. However, considerable uncertainties still remain regarding the dynamics of carbon fluxes over both short and long time scales, and effective strategies are necessary to acquire relevant information about carbon flux processes and to locate and quantify terrestrial sources and sinks of carbon [*Rahman et al.*, 2005]. Since GPP is a measure of carbon uptake by vegetation, an improved knowledge about GPP can provide us with a useful measure of the health of ecosystem and the global carbon cycle.

[3] Estimating GPP of terrestrial ecosystems has been challenging because of its dependence on a variety of environmental factors [*Makela et al.*, 2008]. Among the existing methods, the light use efficiency (LUE) model proposed by *Monteith* [1972] has been widely used [e.g., *Potter et al.*, 1993; *Landsberg and Waring*, 1997; *Coops et al.*, 2005; *Running et al.*, 2000; *Xiao et al.*, 2004; *Yuan et al.*, 2007] to simulate the spatial and temporal dynamics of GPP because of its theoretical basis and practicality [*Running et al.*, 2000]. LUE is defined as the amount of carbon uptake per unit of absorbed photosynthetically active radiation (APAR) by photosynthetic biomass. In LUE, it is assumed that (1) the ecosystem GPP is directly related to the amount of APAR and (2) the actual LUE may be less than its theoretical value because of environmental stresses such as low temperatures or water deficits [*Yuan et al.*, 2007]. The general form of LUE is

$$\mathrm{GPP} = \varepsilon \times \mathrm{fPAR} \times \mathrm{PAR} \tag{1}$$

$$\varepsilon = \varepsilon_{\max} \times f, \tag{2}$$

where PAR is the incident photosynthetically active radiation (MJ $m^{-2}$) per unit time, fPAR is the fraction of incident PAR absorbed by the canopy, $\varepsilon_{\max}$ is the potential

[1]Department of Civil and Environmental Engineering, University of Alberta, Edmonton, Alberta, Canada.


0148-0227/09/2008JG000919$09.00

LUE (g C $m^{-2}$ $MJ^{-1}$ APAR) without environment stress, $f$ is a scalar ranging from 0 to 1 representing the reduction of potential LUE under environmental stresses, fPAR × PAR gives the APAR, and $\varepsilon_{max} \times f$ gives the realized LUE ($\varepsilon$).

[4] In recent years, carbon fluxes measured by the eddy covariance (EC) tower sites set up over forest, grasslands, savannas, etc., have provided useful field measurements for us to parameterize and to validate GPP models. Furthermore, it has been shown that combining these EC tower measurements with remotely sensed (RS) data has the potential to enhance modeling of GPP based on LUE. The MODIS-GPP Algorithm [*Running et al.*, 2004], Vegetation Photosynthesis Model [*Xiao et al.*, 2004], EC-LUE [*Yuan et al.*, 2007], etc., are some examples of successful application of RS data in GPP modeling. The objective of this study is to investigate the applicability of several RS variables in GPP modeling, and to develop a solely RS data–based GPP prediction model that does not depend on any supplementary meteorological data.

## 2. Review of Gross Primary Production Models

[5] The Moderate Resolution Imaging Spectroradiometer (MODIS) sensor onboard the Terra and Aqua satellites provides GPP product (MOD 17) using the LUE method and inputs from the MODIS LAI/fPAR (MOD15A2) product, land cover, and biome-specific climatologic data from NASA's Data Assimilation Office (DAO). In this model, the light use efficiency ($\varepsilon$) is calculated as

$$\varepsilon = \varepsilon_{max} \times m(T_{min}) \times m(\mathrm{VPD}), \tag{3}$$

where $m(T_{min})$ and $m$(VPD) are multipliers that reduce $\varepsilon_{max}$ when cold temperatures and high vapor pressure deficit (VPD), respectively, limit photosynthesis. These factors range linearly from 0 to 1 where 1 denotes no inhibition and 0 denotes total inhibition. Values of $\varepsilon_{max}$, $m(T_{min})$, and $m$(VPD) are listed in the Biome Properties Look-Up Table (BPLUT). By comparing the MODIS GPP product with EC tower estimated GPP across a range of biomes, *Heinsch et al.* [2006] identified three potential sources of errors: (1) errors in meteorological input data derived from NASA's Goddard Earth Observing System (GEOS 4) climate model, (2) errors in MODIS LAI/fPAR product, and (3) errors in the land cover classification.

[6] The Vegetation Photosynthesis Model (VPM) is another LUE model developed by *Xiao et al.* [2004] to estimate GPP using PAR, Enhanced Vegetation Index (EVI), Land Surface Water Index (LSWI) and coarse-resolution temperature data according to equation (1). In VPM, $\varepsilon$ is computed as

$$\varepsilon = \varepsilon_{max} \times T_{scalar} \times W_{scalar} \times P_{scalar}, \tag{4}$$

where $T_{scalar}$, $W_{scalar}$, $P_{scalar}$ are scalars to account for the effects of temperature, water, and leaf age, respectively, on $\varepsilon_{max}$. For this GPP model, it is critical to measure PAR accurately at large spatial scale because PAR is highly variable spatially.

[7] *Sims et al.* [2006] developed a simple model with EVI as the only predictor, but it estimated GPP that were as good or even better than the MODIS GPP product for some sites during periods of active photosynthesis. However, this model gave poor GPP estimates for sites subjected to summer drought or sites dominated by evergreen vegetation. *Sims et al.* [2008] improved this model by adding an additional predictor, Land Surface Temperature (LST). This new model (Temperature and Greenness (TG) Model) computes GPP (equation (5)) for a 16 day period.

$$\mathrm{GPP} = \mathrm{scaledLST} \times \mathrm{scaledEVI} \times m, \tag{5}$$

where $m$ is a scalar,

$$\mathrm{scaledLST} = \min\left[\left(\frac{\mathrm{LST}}{30}\right); (2.5 - (0.05 \times \mathrm{LST}))\right] \tag{6}$$

$$\mathrm{scaledEVI} = \mathrm{EVI} - 0.1. \tag{7}$$

[8] The Global Production Efficiency Model proposed by *Prince and Goward* [1995] also uses APAR to calculate the global GPP using equation (1), but its $\varepsilon$ is based on

$$\varepsilon = \varepsilon_{max} \times T_s \times \mathrm{SM} \times \mathrm{VPD}, \tag{8}$$

where $T_s$ is the soil temperature and SM is the soil moisture index.

[9] The C-Fix model of *Veroustraete et al.* [2002], driven by temperature, radiation and fPAR, assumes that $\varepsilon = \varepsilon_{max}$, which is a fixed value (1.1 g C $m^{-2}$ $MJ^{-1}$ APAR) for calculating GPP (equation (9)), while others [e.g., *Yuan et al.*, 2007] suggest reducing $\varepsilon_{max}$ to $\varepsilon$ under limiting environmental conditions.

$$\mathrm{GPP} = p(T_{atm}) \times \mathrm{CO_{2fert}} \times \varepsilon \times \mathrm{fPAR} \times c \times S_{g,d}, \tag{9}$$

where $p(T_{atm})$ is the normalized temperature dependency factor (value = 0 to 1), $CO_2$fert is the normalized $CO_2$ fertilization factor (value = 1 for no fertilization, and value >1 for fertilization), $c$ is the climate efficiency factor (= 0.48), and $S_{g,d}$ is the daily incoming global solar radiation ($MJ/m^2/d$).

## 3. Research Objectives

[10] Many of the aforementioned GPP models use BPLUT for LUEs and coarse-resolution (e.g., 1° latitude by 1.25° longitude) meteorological inputs that may contain errors and lead to erroneous GPP estimates [*Turner et al.*, 2005; *Zhao et al.*, 2005; *Heinsch et al.*, 2006]. Therefore the objectives of this study are: (1) to develop a GPP model called the "Remotely Sensed-GPP" model (the R-GPP model) without relying on coarse-resolution meteorological variables, but only on four RS variables (two radiation budget variables ($Albedo_{NIR}$ and LST) and two ecosystem variables (Global Vegetation Moisture Index (GVMI) and EVI)); and (2) to assess the transferability of the proposed R-GPP model and its potential to map carbon fluxes of other deciduous forests.

[11] If a dependable GPP model solely relying on RS data can be developed, it may be possible to estimate GPP

accurately at global scale with a spatial resolution the same as that of the satellite data, which for MODIS is 1 km.

## 4. Study Sites and Data Sets

### 4.1. Study Sites

[12] In this study, GPP estimated from three EC towers located in three deciduous forests were used.

[13] 1. The Harvard Forest EC tower (42.54°N, 72.17°W) within the Harvard Forest, Massachusetts, is part of the Ameriflux network and is one of the longest-running tower sites in the world since 1991 [*Goulden et al.*, 1996; *Urbanski et al.*, 2007]. The site primarily consists of 60 to 80 year old deciduous broadleaf forest dominated by red oak, red maple, black birch, white pine, and hemlock [*Goulden et al.*, 1996]. The climate of this forest is temperate, with warm humid summers and annual mean temperature of about 7.9°C, annual precipitation of about 1066 mm, and an average annual plant growing season of about 161 days [*Waring et al.*, 1995].

[14] 2. The Morgan Monroe State Forest (MMSF) EC tower (39.32°N, 86.41°W) of Indiana consists of 60 to 90 year old mixed hardwood forest and is dominated by sugar maple, tulip poplar, white oak, and black oak. Its mean annual temperature is 11.1°C, and mean annual precipitation is 1012 mm [*Curtis et al.*, 2002].

[15] 3. The University of Michigan Biological Station (UMBS) tower (45.56°N, 84.7°W) of Michigan is dominated by 90 year old deciduous forest. Other species are middle-aged conifer, northern hardwood, pine understay, aspen, and hemlock. Its mean annual temperature is 6.2°C, and its mean annual precipitation is 750 mm [*Curtis et al.*, 2002].

### 4.2. Site-Specific Carbon Flux and Climate Data

[16] All the carbon flux data used in this study are means of 8 day period. EC towers do not measure GPP directly, but they measure $CO_2$ exchange between vegetation and the atmosphere in terms of net ecosystem exchange (NEE) using the eddy covariance technique [*Goulden et al.*, 1996]. Then GPP is calculated from the daytime NEE ($NEE_d$) and daytime ecosystem respiration ($R_d$) by

$$GPP = R_d - NEE_d. \quad (10)$$

$R_d$ is usually estimated from daytime temperature and a temperature-respiration relationship usually developed from nighttime NEE measurements that represent nighttime respiration (autotrophic and heterotrophic), because plants do not photosynthesize at night.

### 4.3. Remotely Sensed Data

[17] Among the 36 spectral bands of MODIS, with spatial resolution ranging from 250 m to 1 km [*Justice et al.*, 1998], seven spectral bands are primarily designed for the study of vegetation and land surface: blue (459–479 nm), green (545–565 nm), red (620–670 nm), near infrared (NIR) (841–875 nm, 1230–1250 nm), and shortwave infrared (1628–1652 nm, 2105–2155 nm). MODIS daily surface reflectances are radiometrically calibrated, cloud-filtered, atmospherically corrected for molecular scattering, ozone absorption and aerosols, spatially and temporally gridded, and adjusted for view angle influences. For the three study sites, the 8 day surface reflectance data (MOD09A1, Collection 5) of the four spectral bands, blue, red, NIR (841–875 nm), and shortwave infrared (1628–1652 nm), were collected for 2000–2005 and then used to calculate vegetation indices, EVI, and GVMI.

[18] The other 8 day composite MODIS data sets used in this study include the 1 km LST (MOD11A2, collection 5) and 1 km GPP product (MOD17A2, Collection 5) described in section 2. MOD11A2 is retrieved using the Split-Window algorithm and the thermal infrared bands of MODIS [*Wan and Dozier*, 1996]. We also collected MODIS albedo product, which is produced every 8 days with 16 days of acquisition. The Bidirectional Reflectance Distribution Function (BRDF) coefficients from MCD43A1 were used to calculate the actual albedo for the visible (VIS), NIR, and shortwave bands (0.3–0.7, 0.7–5.0, and 0.3–5.0 $\mu$m, respectively) as a function of optical depth, solar zenith angle, and band [*Schaaf et al.*, 2002; *Lucht et al.*, 2000] (http://daac.ornl.gov/MODIS/MODIS-menu/MCD43.html).

[19] We estimated GPP with 1 km resolution, which is the same as that of MODIS GPP. In other words, we used a 1 km × 1 km area within which the EC tower is located to calibrate the R-GPP model instead of the more common approach of using RS data averaged over of $N \times N$ km area ($N = 3$ or 5, or an even larger number) because the footprint of the EC tower, which depends on the height of flux tower, wind speed, topography, etc., is usually a few hundred meters to 1 km [*Schmid et al.*, 2002; *Xiao et al.*, 2004]. Therefore using predictors averaged over areas of $N \times N$ km in size may be too coarse to represent a tower footprint and may cause a scale mismatch problem between simulated and tower GPP. From this perspective, using RS data at 1 km × 1 km resolution is a better strategy as long as MODIS data have been properly corrected geometrically. Since the RS data are of 1 km (LST and MODIS GPP) and 500 m (reflectance and Albedo) resolutions, for LST and MODIS GPP, we extracted digital values of a 1 km pixel within which the EC tower is located, while for reflectance and albedo, we used the average value of 2 × 2 pixels that represents the same 1 km × 1 km area.

## 5. Research Methodology

[20] The research approach undertaken in this study can be summarized as follows: (1) selecting EVI, GVMI, $Albedo_{NIR}$, and LST as the model predictors and investigating the relationships between these model predictors and few environmental variables such as air temperature, PAR, and VPD, which have been widely used to account for the environmental stresses on GPP; (2) calibrating and validating the R-GPP model using the Harvard Forest tower estimated GPP data of years 2000–2003 and 2004–2005, and comparing its results with the MODIS GPP product (MODIS-17); and (3) testing the transferability of the R-GPP model calibrated for Harvard Forest to two other deciduous forests sites: Morgan Monroe State Forest and University of Michigan Biological Station of United States.

### 5.1. R-GPP Model Predictors

#### 5.1.1. Global Vegetation Moisture Index

[21] Previous studies have demonstrated the possibility of using NIR and short wave infrared bands to retrieve leaf and

**Table 1.** Correlations Between Model Predictors and GPP at the Harvard Forest for 2000–2005

| Predictor | Coefficient of Determination ($R^2$)[a] |
|---|---|
| GVMI | 0.11 |
| GVMI (growing season) | **0.60** |
| $Albedo_{NIR}$ | **0.82** |
| EVI | **0.84** |
| $LST_s$ | **0.71** |

[a]Correlations significant at 1% significant level are shown in bold.

canopy water content (g/m$^2$) using Landsat-TM data [*Hunt and Rock*, 1989], hyperspectral data [*Gao*, 1996; *Serrano et al.*, 2000], and VEGETATION (VGT) sensor data [*Ceccato et al.*, 2001]. Recently, *Ceccato et al.* [2002a, 2002b] proposed to retrieve equivalent water thickness (EWT) at the canopy level using GVMI from the VGT sensor,

$$\mathrm{GVMI} = \frac{(\mathrm{NIR} + 0.1) - (\mathrm{SWIR} + 0.02)}{(\mathrm{NIR} + 0.1) + (\mathrm{SWIR} + 0.02)}, \qquad (11)$$

where NIR and SWIR are reflectance of the rectified NIR band and short wave infrared bands, respectively. *Ceccato et al.* [2002b] tested GVMI in retrieving EWT from four different ecosystems and found that water content retrieved from GVMI was consistent with field measured water content. Other studies also demonstrated the applicability of GVMI in retrieving EWT [e.g., *Danson and Bowyer*, 2004; *Du et al.*, 2005].

[22] To incorporate the effect of water stress in the R-GPP model, we used GVMI computed from MODIS reflectance products. Although GVMI is not correlated with the GPP of Harvard Forest throughout the year (Table 1), they are significantly correlated ($R^2$ = 0.60) during the growing season (mid April to 27 October [*Urbanski et al.*, 2007]) of this deciduous study site. However, in early spring, late fall, and winter, high values of GVMI could still be observed because of snow cover above or below the canopy (Figure 1a). Therefore, during these cold periods, GPP is not related to GVMI but is probably controlled by the LST, which will be explained in section 5.1.4.

[23] Figure 1a (right) shows that GPP increases with GVMI (related to soil moisture) during the growing season. However, Figure 1a (left) also shows that when GVMI is around 0.4 to 0.5, GPP fluctuates widely from 5 to 14, showing little relation to GVMI because when there is sufficient soil moisture (water is not a limiting factor), photosynthesis will probably depend more on temperature, which is related to the incoming solar radiation. *Yuan et al.* [2007] also reported that GPP is controlled either by air temperature or by soil moisture, whichever is the most limiting.

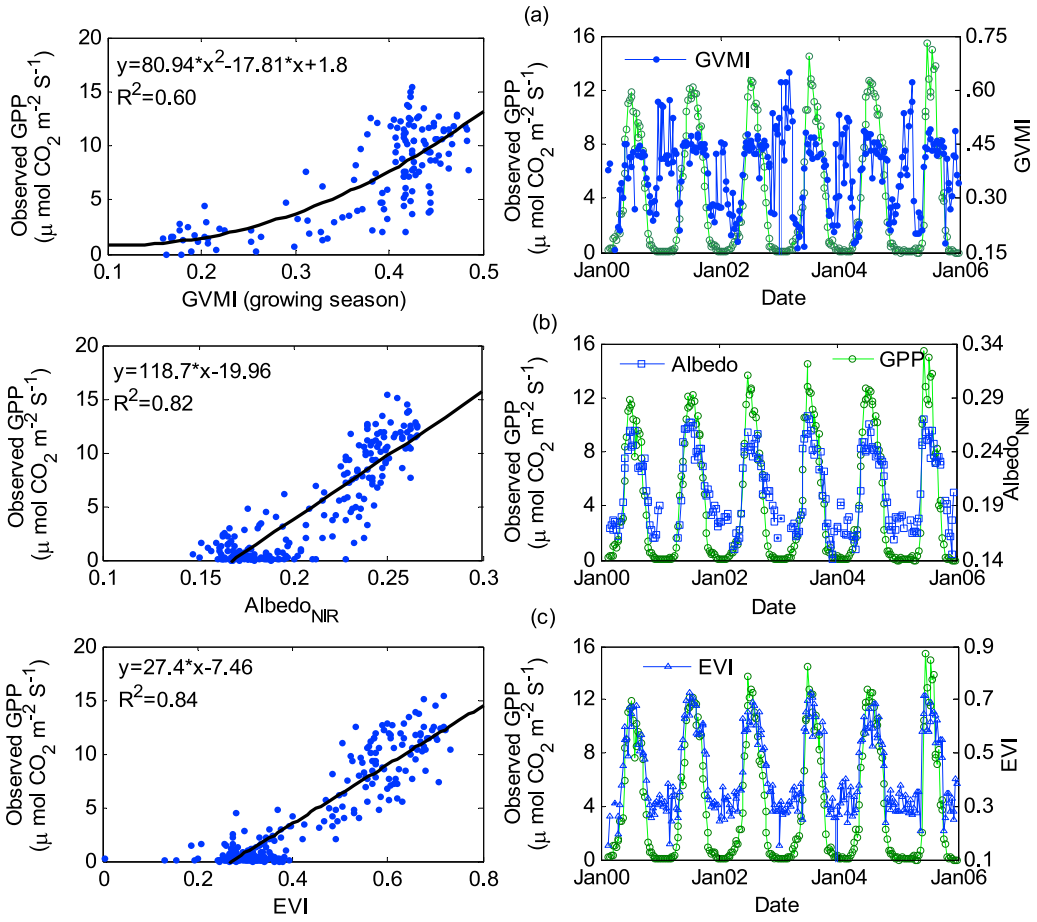


**Figure 1.** (left) Nonlinear/linear regression and (right) comparison of seasonal dynamics between GPP and (a) GVMI, (b) $Albedo_{NIR}$, and (c) EVI for 2000 to 2005 at Harvard Forest. All points represent 8 day means.

#### 5.1.2. Near-Infrared Albedo

[24] Albedo ($\alpha$), the fraction of incident solar radiation reflected by a surface (equation (12)), plays a key role in partitioning the total radiative flux into absorbed, sensible, latent, and reflected fluxes [*Bounoua et al.*, 2000]. The net radiation $R_n$ is given as

$$\begin{aligned} R_{\mathrm{n}} &= S_{\mathrm{in}} - S_{\mathrm{out}} + L_{\mathrm{in}} - L_{\mathrm{out}} \\ &= S_{\mathrm{in}}(1-\alpha) + L_{\mathrm{in}} - L_{\mathrm{out}}, \end{aligned} \tag{12}$$

where $S_{\mathrm{in}}$ and $S_{\mathrm{out}}$ are the incoming and outgoing solar (shortwave) radiation, respectively, and $L_{\mathrm{in}}$ and $L_{\mathrm{out}}$ are the downwelling and upwelling longwave radiation at the surface, respectively.

[25] Albedo influences the radiation absorbed by plant canopies and thereby affects physical and biogeochemical processes such as photosynthesis, energy balance, evapotranspiration, and respiration [*Wang et al.*, 2001, 2002a, 2002b]. Furthermore, surface albedo also affects rainfall, vegetation growth [e.g., *Bounoua et al.*, 2000; *Laval and Picon*, 1986; *Wang and Davidson*, 2007], and even droughts that could lead to desertification [*Dirmeyer and Shukla*, 1996; *Knorr et al.*, 2001]. The albedo of vegetation, unlike that of bare soil, shows temporal variability due to the seasonal behavior of plant phenology such as green-up, peak greenness, dry-down, and senescence. For example, *Song* [1998] found that the albedo of a wheat field decreased from the peak green to senescence stage. Although some previous studies on GPP [e.g., *Ichii et al.*, 2003; *Landsberg and Waring*, 1997; *Gebremichael and Barros*, 2006; *Kimball et al.*, 1997] used albedo to calculate radiative fluxes, as far we know, none of them reported a direct relationship between NIR albedo and GPP, and most of these models used a constant albedo without considering its temporal variability.

[26] In this study, albedo at the NIR band, $\mathrm{Albedo_{NIR}}$ (0.7 to 5 $\mu$m) has been used because the reflectance of vegetation is very strong at NIR band, and likely because of this, it is the most commonly used albedo in ecosystem modeling [*Wang and Davidson*, 2007; *Ghulam et al.*, 2007; *Ollinger et al.*, 2008]. Since only 16 day resolution albedo data are available from MODIS, we have used that 16 day albedo product produced every 8 days (e.g., albedo of date 1 corresponds to average albedo of days 1 to 16 while albedo of date 9 corresponds to average albedo of days 9 to 24). To estimate the GPP of any 8 day period, we have used $\mathrm{Albedo_{NIR}}$ averaged over those particular 8 days and the previous 8 days while the other predictors were averaged over those particular 8 days. For example, to calculate the average GPP of days 9 to 16 (17 to 24), we have used the average albedo of days 1 to 16 (9 to 24) while the other predictors were averages of days 9 to 16 (17 to 24). Therefore the R-GPP remains as an 8 day GPP model.

[27] Table 1 and Figure 1b show that the seasonal dynamics of $\mathrm{Albedo_{NIR}}$ and GPP are strongly correlated with each other for the Harvard Forest site with a $R^2 = 0.82$ for the 2000–2005 data, which indicates that using only $\mathrm{Albedo_{NIR}}$, GPP may be modeled with comparable or better accuracy than the GPP estimates from MODIS ($R^2 = 0.78$ for 2000–2005) for this site. $\mathrm{Albedo_{NIR}}$ gradually increases with the green-up of deciduous forest because of the high reflectance of canopy leaves in the NIR band and continues until the peak green stage and then gradually decreases with the senescence of leaves (Figure 1b, right), as was also observed by *Wang* [2005] for a boreal deciduous forest of Saskatchewan, Canada.

#### 5.1.3. Enhanced Vegetation Index

[28] EVI produces vegetation signal with improved vegetation monitoring through canopy background and atmospheric corrections [*Waring et al.*, 2006]. It is more sensitive than the popular normalized difference vegetation index (NDVI) in high biomass regions.

$$\mathrm{EVI} = G\frac{\mathrm{NIR} - R}{\mathrm{NIR} + C_1 R - C_2 B + L}, \tag{13}$$

where NIR, $R$, and $B$ are atmospherically corrected surface reflectance in the near-infrared, red, and blue bands, respectively; $G$ is the gain factor; $L$ is the canopy background adjustment factor that addresses nonlinear, differential NIR and red radiant transfer through a canopy; and $C_1$ and $C_2$ are the coefficients of the aerosol resistance term, which uses the blue band to correct the aerosol influences in the red band. In the EVI algorithm, $L = 1$, $C_1 = 6$, $C_2 = 7.5$, and $G = 2.5$. EVI has been shown to be a good predictor of growing season GPP for many sites and it was used as a predictor in some previous models [*Xiao et al.*, 2004]. In this study we found that the seasonal dynamics of GPP agrees reasonably well with EVI ($R^2 = 0.84$) for the Harvard Forest (Figure 1c) and so EVI was selected as a predictor.

#### 5.1.4. Land Surface Temperature

[29] LST is a potential predictor for GPP estimation because it can incorporate the effect of temperature and VPD on vegetation [*Hashimoto et al.*, 2008]. It is highly correlated with vegetation dynamics [*Sun and Kafatos*, 2007] and is positively correlated with NDVI in high latitudes [*Karnieli et al.*, 2006]. *Boegh et al.* [1999] found the slope of LST/NDVI to be related to the evapotranspiration of Sahel.

[30] The scatterplot of GPP with LST (Figure 2a) shows that below 0°C, there is no photosynthesis while above 0°C, GPP slowly increases with LST, which implies that 0°C can be used as a temperature threshold for this deciduous forest to define periods of active photosynthesis. Some studies [*Sims et al.*, 2008; *Yuan et al.*, 2007] reported that photosynthesis is predominantly controlled by temperature only at the beginning and the end of a growing season, but by moisture conditions throughout the growing season. Therefore we used a scaled LST ($\mathrm{LST_s}$) (equation (14)) to set GPP to zero when LST is below 0°C.

$$\begin{aligned} \mathrm{LST_s} &= \frac{\mathrm{LST}}{\mathrm{LST_{max}}} \quad \text{for} \quad \mathrm{LST} > 0^{\circ}\mathrm{C} \\ \mathrm{LST_s} &= 0 \qquad\quad \text{for} \quad \mathrm{LST} \le 0^{\circ}\mathrm{C}, \end{aligned} \tag{14}$$

where LST is the observed LST and $\mathrm{LST_{max}}$ is the maximum LST. In this study, $\mathrm{LST_{max}}$ is set to 30°C partly because it has been used as the optimum LST in some other studies [*Sims et al.*, 2008]. Figure 2b shows that GPP is strongly correlated with $\mathrm{LST_s}$ ($R^2 = 0.71$). Throughout the summer, GPP increases with increasing

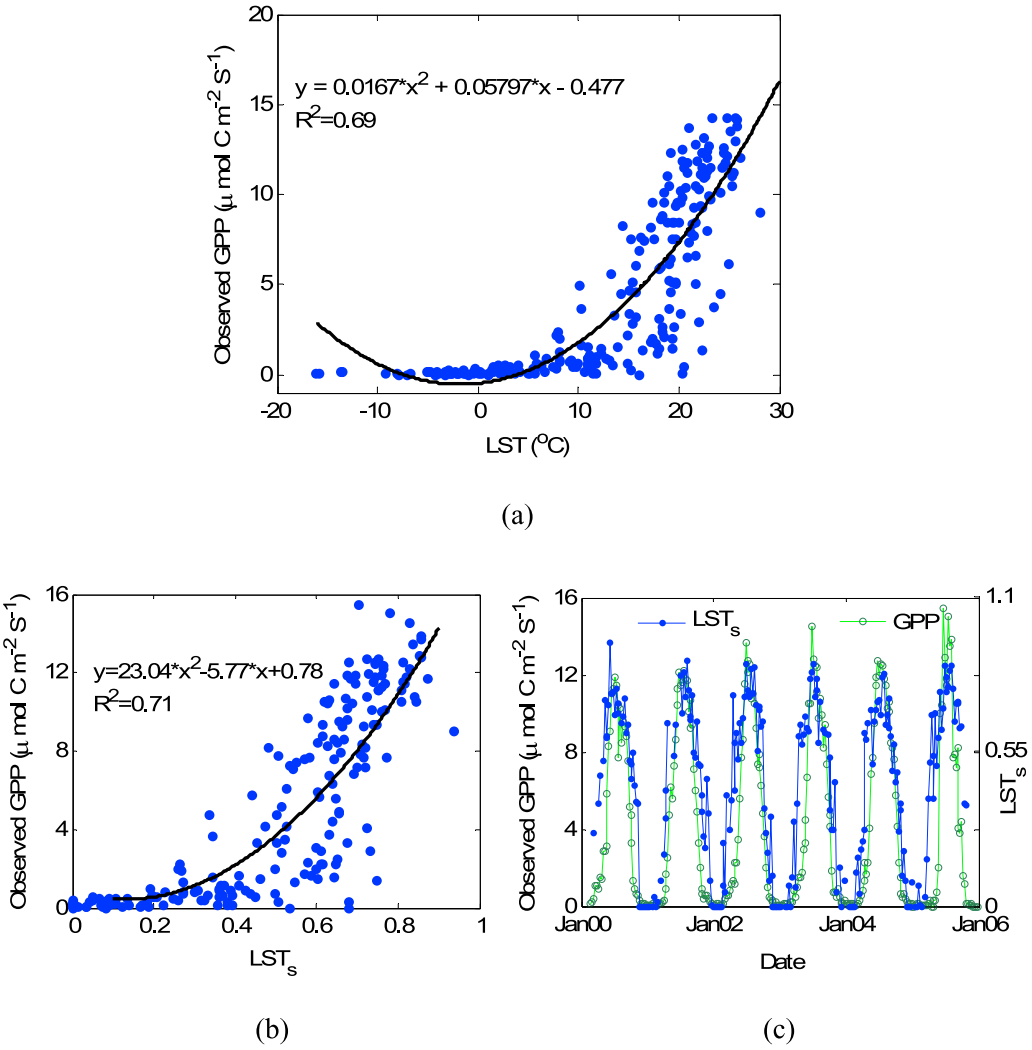


**Figure 2.** Scatterplot and polynomial fit between GPP and (a) LST and (b) scaled LST ($LST_s$), and (c) seasonal dynamics of GPP and $LST_s$ for 2000 to 2005 at the Harvard Forest. All points represent 8 day means.

$LST_s$; but as the season enters into fall, $LST_s$ decreases and GPP drops because the deciduous forest slowly drops its leaves (Figure 2c). However, it is also found that GPP does not respond instantaneously with temperature rise during the early growing season (at low $LST_s$), which is attributed to the lag in the leaf development of deciduous forest in the spring (Figures 2b and 2c). Furthermore, low $LST_s$ during the start and the end of each growing season restricts water and nutrient uptake and hence it affects photosynthesis [*Sims et al.*, 2008].

### 5.2. Relationships Between Model Predictors and Other Environmental Variables

[31] The relationships between the R-GPP model predictors (EVI, $LST_s$, GVMI, and $Albedo_{NIR}$) and some environmental variables (PAR, VPD, and air temperature) measured at the EC tower site of Harvard Forest were examined. These environmental variables have been popular predictors of carbon flux, but they vary substantially over space and usually are only available as limited ground measurements or coarse-resolution, gridded data. Therefore, if we can establish meaningful relationships between PAR, air temperature, VPD, and aforementioned RS predictors, it will be possible to get a continuous estimation of carbon fluxes on the basis of RS predictors as they are acquired on a continuous basis.

[32] PAR was found to be reasonably correlated with the R-GPP model predictors for 2000 to 2005 (Table 2 and Figure 3). As GVMI influences photosynthesis only in the active photosynthesis period, and during nonactive period (winter) it is affected by snow cover above or below the canopy, the seasonal cycle of GVMI and PAR did not match

**Table 2.** Correlations Between Model Predictors and Different Environmental Variables for 2000–2005 at Harvard Forest

| | Coefficient of Determination ($R^2$)[a] | | | |
|---|---|---|---|---|
| Variables | GVMI | $Albedo_{NIR}$ | EVI | $LST_s$ |
| PAR | 0.02 | **0.47** | **0.46** | **0.64** |
| Tair | 0.01 | **0.67** | **0.64** | **0.92** |
| VPD | 0.01 | **0.30** | **0.29** | **0.60** |

[a]Correlations significant at 1% significant level are shown in bold.

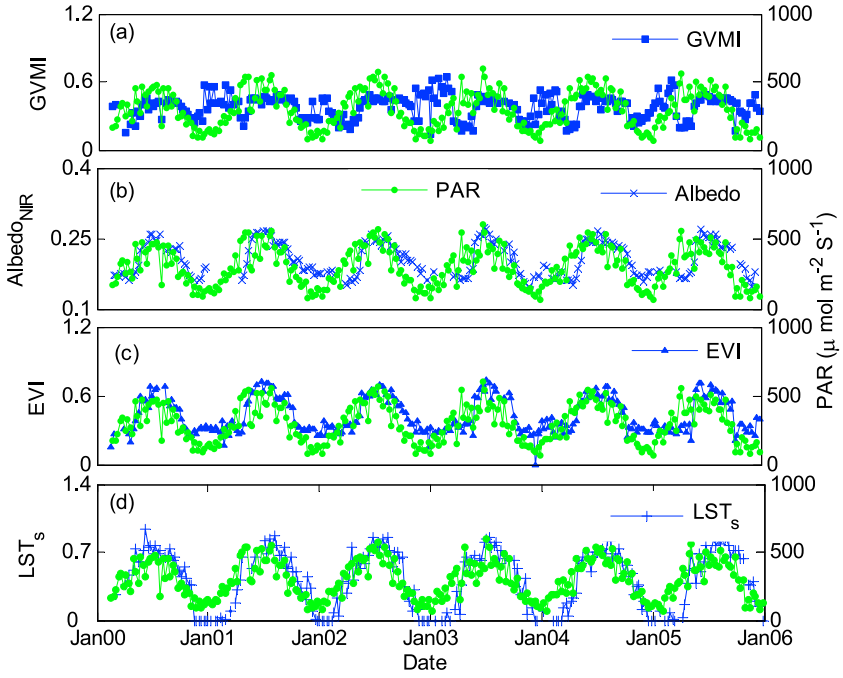


**Figure 3.** Comparison of seasonal dynamics of photosynthetically active radiation (PAR) with seasonal dynamics of (a) GVMI, (b) Albedo$_{NIR}$, (c) EVI, and (d) LST$_s$ for 2000 to 2005 at Harvard Forest. All points represent 8 day means.

during winter and the overall correlation between PAR and GVMI was relatively poor (Table 2). However, LST$_s$, EVI, and Albedo$_{NIR}$ followed the seasonal variation of PAR quite systematically, which implies that these variables can possibly replace PAR, which is one of the most critical predictors in the estimation of GPP [*Xiao et al.*, 2004].

[33] EVI, Albedo$_{NIR}$, and LST were also found to be consistently correlated with air temperature ($T_{air}$) (Figure 4) and VPD (Figure 5), which have been key predictors in many GPP models [*Yuan et al.*, 2007]. Since the correlation between $T_{air}$ and LST$_s$ is very high ($R^2$ = 0.92), it likely means that LST$_s$ can replace $T_{air}$. Moreover, using LST$_s$

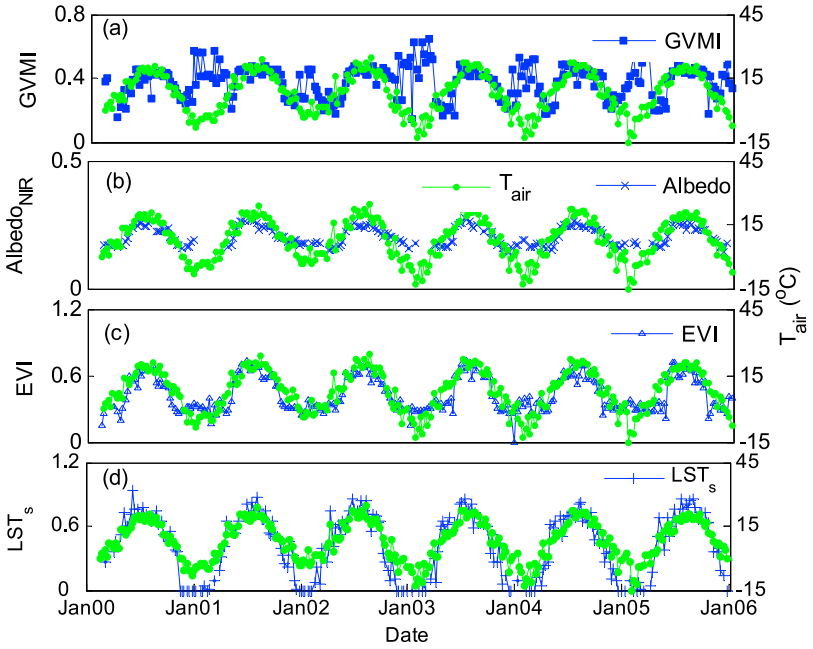


**Figure 4.** Comparison of seasonal dynamics of air temperature ($T_{air}$) with seasonal dynamics of (a) GVMI, (b) Albedo$_{NIR}$, (c) EVI, and (d) LST$_s$ for 2000 to 2005 at Harvard Forest. All points represent 8 day means.

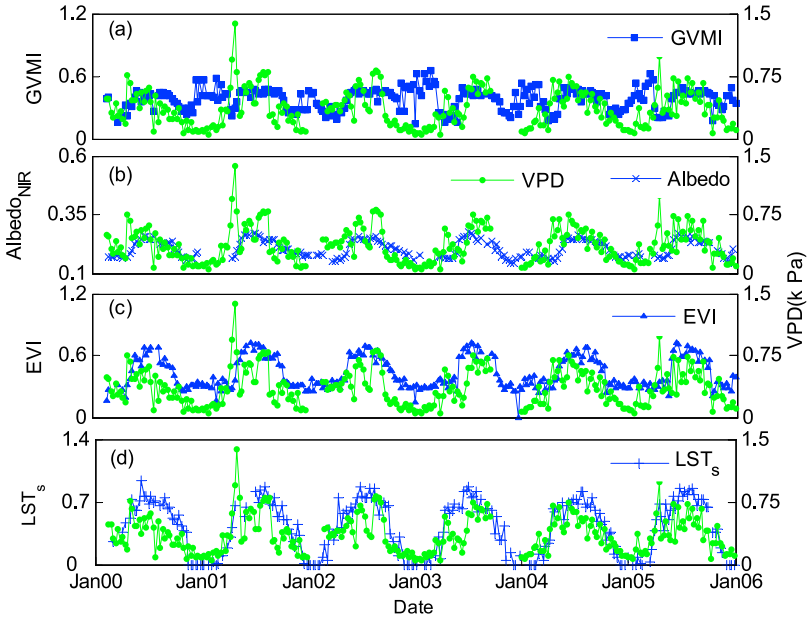


**Figure 5.** Comparison of seasonal dynamics of vapor pressure deficits (VPD) with seasonal dynamics of (a) GVMI, (b) $Albedo_{NIR}$, (c) EVI, and (d) $LST_s$ for 2000 to 2005 at Harvard Forest. All points represent 8 day means.

instead of $T_{air}$ will allow us to use data of fine spatial resolution instead of limited ground measured data from climate stations or coarse-resolution data simulated from global climate models (e.g., NASA's Data Assimilation Office GEOS 4 global climate model). The high values of GVMI because of snow cover effects during winter weakened the overall correlation (Table 2) of GVMI with $T_{air}$ and VPD (Figure 5a). Given that GPP is controlled by LST during winter, the poor correlation of GVMI with GPP and other environmental variables during winter may only have marginal effect on the winter GPP simulated by the R-GPP model.

## 6. R-GPP Model Development and Results

[34] Given that GVMI, EVI, $Albedo_{NIR}$, and LSTs are correlated to GPP and to PAR, VPD, and air temperature, which are key elements of many GPP models, we propose a remotely sensed GPP (R-GPP) model (equation (15)) based on these four RS predictors only,

$$GPP = k \times GVMI^a \times LST_s^b \times Albedo_{NIR}^c \times EVI^d, \qquad (15)$$

where $k$ is a scalar, and $a$, $b$, $c$, and $d$ are exponents. These model parameters were estimated using the estimated GPP of 2000 to 2003 from the EC tower located at the Harvard Forest site and a nonlinear optimization scheme, the Generalized Reduced Gradient (GRG2) [*Lasdon et al.*, 1978; *Spaulding*, 1998]. By GRG2, the optimized values of $k$, $a$, $b$, $c$, and $d$ have been found to be 114, 0.885, 1.05, 0.695, and 0.933, respectively.

[35] The performance of R-GPP was evaluated in terms of the coefficient of determination ($R^2$) and root-mean-square error (RMSE). The calibration results show that R-GPP model could capture the seasonal dynamics of the observed GPP accurately (Figure 6 and Figure 7a (left) and Table 3). With respect to the EC tower estimated GPP, it is clear that R-GPP ($R^2 = 0.95$, RMSE = 1.02 $\mu$mol C/m$^2$/s) was more efficient than the MODIS GPP algorithm ($R^2$ = 0.80, RMSE = 2.78 $\mu$mol C/m$^2$/s) for the Harvard Forest site, especially during the peak growing season. In almost all years tested, the MODIS algorithm showed a marginal overestimation in the early part of the plant growing season and an underestimation in the peak growing season (June to September) (Figure 7b (left), as was also reported by *Xiao et al.* [2004] for the Harvard Forest site. The poor estimate of MODIS-GPP likely arises from uncertainties related to meteorological inputs, and from erroneous land cover classification and LAI/fPAR product [*Heinsch et al.*, 2006] used in the MODIS algorithm (as explained in section 2). Moreover, $\varepsilon_{max}$ used in the MODIS GPP algorithm, which is

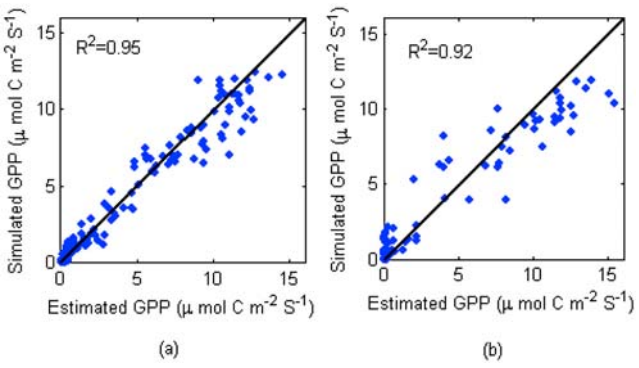


**Figure 6.** Scatterplot of R-GPP model simulated gross primary production (GPP) and eddy covariance tower estimated GPP for the (a) calibration (2000–2003) and (b) validation stages (2004–2005) at the Harvard Forest site. All points represent 8 day means.

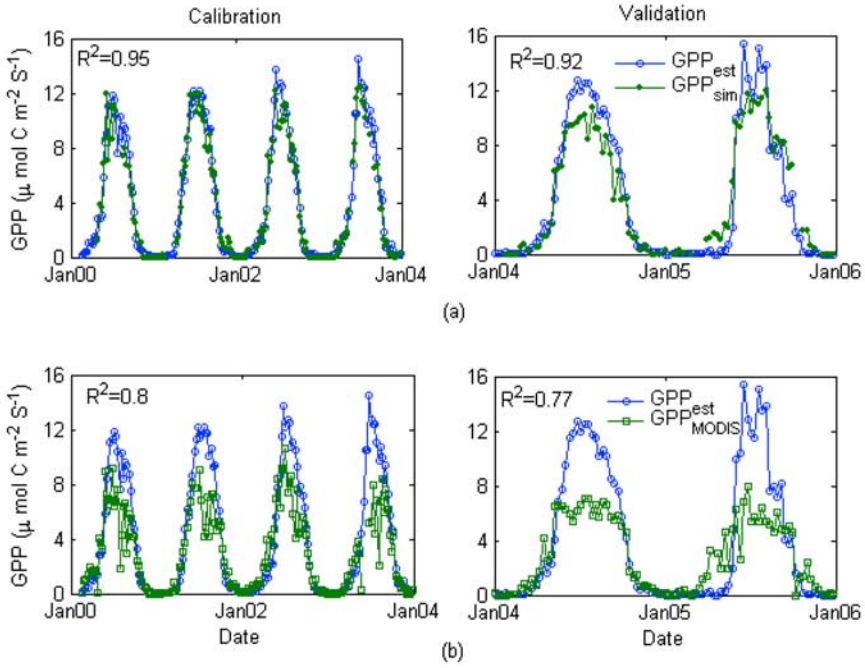


**Figure 7.** Annual cycle of eddy covariance tower estimated gross primary production ($GPP_{est}$) and (a) R-GPP model predicted GPP ($GPP_{sim}$) and (b) MODIS GPP ($GPP_{MODIS}$) product for the Harvard Forest site during (left) the calibration (2000–2003) and (right) validation stages (2004–2005). All points represent 8 day means.

biome specific, has been found to be smaller than the $\varepsilon_{max}$ value observed at the Harvard Forest [*Turner et al.*, 2003]. Using an underestimated $\varepsilon_{max}$ may cause an underestimated GPP.

[36] The calibrated R-GPP model ($R^2$ = 0.92, RMSE = 1.62 $\mu$mol C/m$^2$/s) also outperformed the MODIS GPP algorithm ($R^2$ = 0.77, RMSE = 3.35 $\mu$mol C/m$^2$/s) in the validation stage (2004–2005) of the Harvard Forest. The MODIS GPP algorithm underpredicted the EC tower GPP quite substantially during the growing season (Figure 7b, right) of 2004–2005 whereas the R-GPP model's prediction was relatively close to the EC tower GPP (Figure 7a, right).

[37] Even though the overall simulated GPP of the R-GPP model closely matched the observed, occasionally there were large discrepancies between them (especially in the validation stage), partly because of the limitations of R-GPP and possibly because of the error in the observed GPP estimated from $NEE_d$ and $R_d$, which are subjected to uncertainties [*Xiao et al.*, 2004]. Moreover, there are gaps in both NEE and $R_d$ data, and gap-filling steps of these data are still subjected to debates [*Falge et al.*, 2001]. Therefore, even though the gap-filled "estimated GPP" data can be used to assess the performance of GPP models reasonably accurately, some uncertainties are expected.

## 7. Transferability of R-GPP Model

[38] Given that EC towers are established only in limited sites, it will be useful to examine the transferability of the proposed R-GPP model calibrated for the Harvard Forest site to other deciduous forests located in northeastern United States to estimate their carbon fluxes. Intuitively, the degree of transferability will depend on the degree of similarity in terms of vegetation types and climate regimes and how accurately the four predictors (GVMI, $Albedo_{NIR}$, EVI, and $LST_s$) measure the basic environmental properties such as moisture condition, reflectivity, and surface temperature. *Gilmanov et al.* [2005] argued that models based on vegetation indices such as NDVI (and presumably EVI) are transferable as long as vegetation types and age are comparable between the sites, since these are two important factors to be considered in estimating GPP [*Desai et al.*, 2008]. To test its transferability, the R-GPP model developed out of the Harvard Forest site was applied to UMBS and MMSF forest sites, which are also mature deciduous forests with stand age 60 to 90 years.

[39] Figure 8a (left) shows that the R-GPP model developed for the Harvard Forest simulated the observed GPP of MMSF more accurately ($R^2$ = 0.93, RMSE = 1.47 $\mu$mol

**Table 3.** Correlation Between Observed GPP and Either R-GPP Model Predicted GPP or MODIS GPP[a]

| | | Observed GPP Versus Simulated GPP (R-GPP Model) | | Observed GPP Versus MODIS GPP | |
|---|---|---|---|---|---|
| Site | Study Period | $R^2$ | RMSE | $R^2$ | RMSE |
| Harvard Forest | 2000–2003 (Calibration) | 0.95 | 1.02 | 0.80 | 2.78 |
| | 2004–2005 (Validation) | 0.92 | 1.62 | 0.77 | 3.35 |
| MMSF | 2000–2005 | 0.93 | 1.47 | 0.74 | 3.54 |
| UMBS | 2000–2003 | 0.94 | 0.95 | 0.91 | 1.48 |

[a]All GPP are mean values of 8 day periods. Correlation is $R^2$. Unit of RMSE is $\mu$mol C/m$^2$/s.

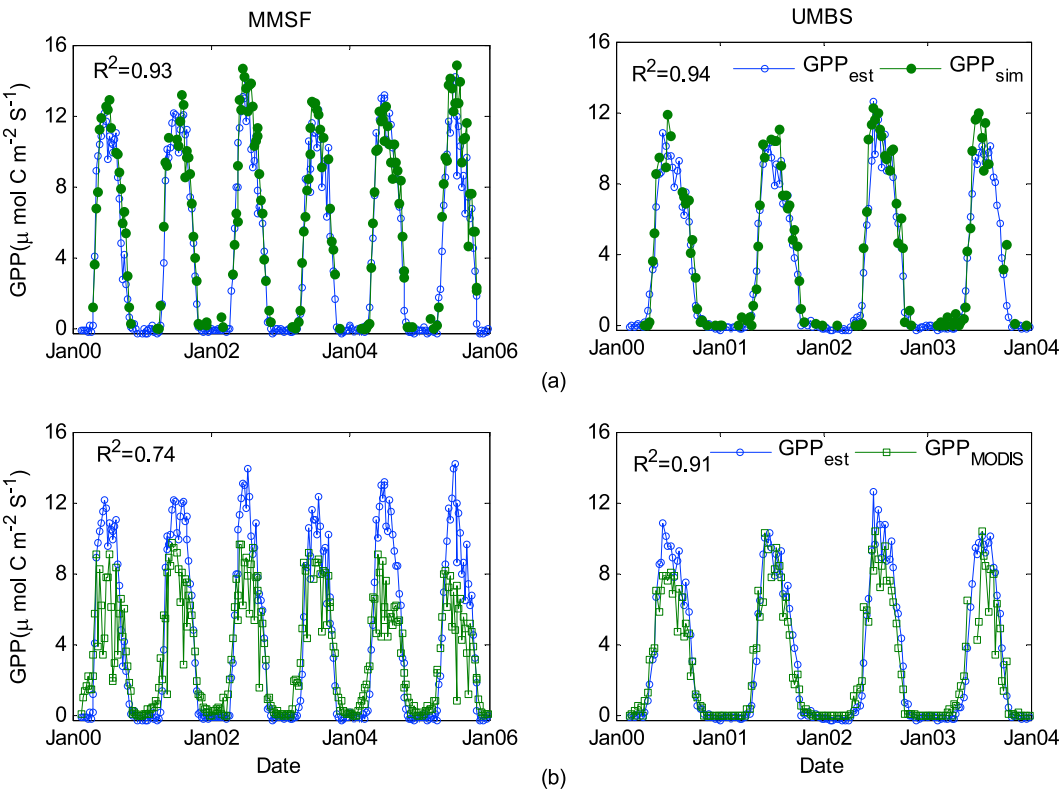


**Figure 8.** Annual cycle of eddy covariance tower estimated gross primary production ($GPP_{est}$) and (a) R-GPP model predicted GPP ($GPP_{sim}$) and (b) MODIS GPP ($GPP_{MODIS}$) product for (left) the Morgan Monroe State Forest (MMSF) during 2000–2005 and (right) University of Michigan Biological Station Site (UMBS) during 2000–2003. All points represent 8 day means.

$C/m^2/s$) than the MODIS GPP algorithm ($R^2$ = 0.74, RMSE = 3.54 $\mu$mol $C/m^2/s$). The MODIS GPP algorithm consistently showed an underestimation in the peak growing season for most of the years (2000–2005) and an overestimation in the early growing seasons for some years (Figure 8b, left). In contrast, the R-GPP model only showed minor overestimation during the peak growing season of 2000–2002 and marginal underestimation in 2004.

[40] For the UMBS site, the R-GPP model's predicted GPP also followed the seasonal dynamics of the observed GPP very well (Figure 8a, right), and the agreement is marginally better than the GPP estimated by the MODIS algorithm, for example, $R^2 = 0.94$ versus $R^2 = 0.91$ (Table 3). On the whole, for UMBS, the MODIS GPP product showed better estimation during the early growing season and peak season (Figure 8b, right) than it did for the other two sites.

[41] Given that both UMBS and MMSF test sites are located more than about 1000 km away from the Harvard Forest, it seems that the proposed R-GPP model using the four selected RS predictors can generally estimate the GPP of deciduous forests located at the northeastern United States. Even though simple in nature and built on the basis of the RS data only, the R-GPP model possesses the necessary physical basis to capture the basic ecological and environmental functioning of deciduous ecosystems, which is probably why R-GPP turns out to be more effective than the MODIS GPP in characterizing the seasonal variability of GPP of three deciduous ecosystems of northeastern United States.

## 8. Discussion

[42] In recent years, RS data–based models have demonstrated strong potential in GPP modeling, for example, MODIS GPP algorithm [*Running et al.*, 2004], TG model [*Sims et al.*, 2008], VPM [*Xiao et al.*, 2004], MOD-SIM-Cycle [*Hazarika et al.*, 2005], and EC-LUE [*Yuan et al.*, 2007]. Our proposed R-GPP model is different from other GPP models because it is dependent solely on RS data, whereas the majority of the RS-based models (e.g., MODIS GPP) require supplementary meteorological inputs that are often available with spatial resolutions poorer than the RS variables, and as a result may produce significant errors in regional scale GPP estimation [*Heinsch et al.*, 2006]. Our proposed R-GPP model is likely closest to the TG model of *Sims et al.* [2008], which is also solely RS data based. However, the R-GPP model estimates 8 day means of GPP while the TG model computes 16 day means of GPP using EVI and LST, as described before.

[43] Although the overall performance of the R-GPP model was encouraging, there are still discrepancies when compared with field observations, especially for the Harvard Forest during the growing season of the validation period. The surface reflectance products from 8 day composite images are likely a key factor that may affect the

accuracy of GPP predicted by the R-GPP model. The compositing method (e.g., currently MODIS reflectance data is composited on the basis of a minimum-blue criterion that selects the clearest conditions over the period) could result in some bias, so EVI and GVMI computed from the reflectance products may not reflect the average condition of that 8 day period [*Xiao et al.*, 2004]. Therefore GPP estimated by the R-GPP model may differ from the observed 8 day mean GPP. This problem can be partly resolved by using daily images as input to the R-GPP model, although this would incur large increases in computer processing.

[44] Another factor that may affect the results of the R-GPP model is the 16 day albedo of MODIS. To estimate the GPP of any 8 day period, the R-GPP model uses $Albedo_{NIR}$ averaged over that particular 8 days and the previous 8 days (section 5.1.2). This averaging may introduce some discrepancies. Moreover, the nutrition limit is not explicitly considered in the R-GPP model, which partly contributed to the discrepancies between the R-GPP model output and that estimated from the EC tower.

[45] This study demonstrated that combining indices such as GVMI, EVI, $Albedo_{NIR}$, etc., in a meaningful manner can capture the temporal dynamics of photosynthetic activities of deciduous ecosystems in northeastern United States. GVMI and EVI enabled us to account for the soil moisture state and the overall status of vegetation, while albedo and LST provided crucial information about the surface energy necessary for plant growth [*Huete*, 2005]. This study has demonstrated the applicability of these predictors and their quantitative relationships with GPP. It may be useful to examine other vegetation indices (e.g., the normalized difference water index) to more comprehensively model the seasonal dynamics of GPP across different ecosystems.

[46] At present about 400 EC tower sites are operating worldwide, under the FLUXNET network, on a continuous and long-term basis to collect information on carbon, moisture, and energy fluxes (http://daac.ornl.gov/FLUXNET/). These towers are located in different parts of the world and belong to different climatic regimes. Multiyear GPP data from EC towers located in various deciduous forests can be used to validate the R-GPP model. However, some of these flux data are not yet publicly available, because the analysis and publications of flux data are time consuming [*Xiao et al.*, 2004]. When data from many EC tower sites become publicly available, we will be in a better position to more comprehensively validate this R-GPP model, to better identify various sources of error, and to fine tune the model.

[47] The time scale of the R-GPP model is dictated by the temporal resolution of the MODIS data. Among the four model predictors, albedo is not available on a daily basis, and so it is not possible to compute daily GPP using the R-GPP model, which for now can only operate at an 8 day period. Some LUE based models [e.g., *Yuan et al.*, 2007; *Makela et al.*, 2008] can be used to model daily GPP variations, which, however, depend on meteorological data whose limitations have already been discussed in section 2.

## 9. Summary and Conclusions

[48] We have developed a GPP estimation model, called the R-GPP model, solely based on four remotely sensed (RS) variables, namely the EVI, near-infrared albedo, GVMI, and LST as model predictors. The model was calibrated (2000–2003) and validated (2004–2005) on the basis of GPP estimated from fluxes of an eddy covariance tower located in the Harvard Forest, United States. The summary of the results are listed below.

[49] 1. The proposed model predicted the GPP of the Harvard Forest accurately, with $R^2 = 0.95$ and $R^2 = 0.92$ in the calibration and the validation periods, respectively, which is much better than the MODIS-GPP algorithm ($R^2 = 0.80$ and $R^2 = 0.77$ in the calibration and validation stages, respectively) even though the latter is relatively complex and requires meteorological inputs which are mostly available in coarse resolution only.

[50] 2. The model predictors individually showed strong correlation to the GPP of the Harvard Forest for 2000–2005 ($R^2 = 0.60$, 0.84, 0.82, and 0.71 for GVMI (during growing season), EVI, $Albedo_{NIR}$, and $LST_s$, respectively). Furthermore, for the Harvard Forest, the $Albedo_{NIR}$ or the EVI itself could predict GPP marginally better than the MODIS GPP ($R^2 = 0.78$ for 2000–2005). Therefore, the R-GPP model outperformed the MODIS-GPP algorithm since it is designed to take the advantage of the combined contributions of all these four RS predictors.

[51] 3. The R-GPP model predictors, such as EVI, $Albedo_{NIR}$, and LST, have been shown to be correlated with a few other environmental variables such as air temperature, PAR, and VPD, which have been widely used as predictors in modeling GPP. The relationships between them imply that the predictors of R-GPP model, which are available in relatively fine spatial resolutions, can replace meteorological predictors of coarse spatial resolutions in GPP modeling.

[52] 4. The transferability of the R-GPP model, calibrated for the Harvard Forest, was tested by applying it to two other deciduous forest sites, MMSF and UMBS. The R-GPP model captured the seasonal dynamics of the observed GPP of MMSF ($R^2 = 0.93$) and UMBS ($R^2 = 0.94$) more accurately than the MODIS GPP algorithm ($R^2 = 0.74$ and $R^2 = 0.91$ for MMSF and UMBS, respectively). Apparently the R-GPP model is transferable and can estimate the GPP of other similar deciduous forests, especially those that are located in northeastern United States.

[53] Although the proposed R-GPP model has shown promising results in estimating GPP of several deciduous forests of northeastern United States, further validation is needed to test the robustness of the R-GPP model and its applicability in different climatic and biophysical conditions. The model parameters may need to be refined for other climatic regimes and biomes. Further study is also needed to determine whether net primary production can be estimated from the RS variables used in this study.

[54] **Acknowledgments.** The gap-filled carbon flux and climate data of University of Michigan Biological Station (UMBS) and Morgan Monroe State Forest (MMSF) sites were collected from the Ameriflux website (http://public.ornl.gov/ameriflux/) for 2000–2003 and 2000–2005, respectively, while data for the Harvard Forest [*Urbanski et al.*, 2007] were obtained from the data archive (ftp://ftp.as.harvard.edu/pub/nigec/HU_Wofsy/hf_data/Final/Filled) for 2000–2005. We wish to thank the researchers who worked at the eddy covariance tower of Harvard Forest, MMSF, and UMBS sites. The MODIS data were collected from the Oak Ridge National Laboratory's (ORNL) Distributed Active Archive Centre (DAAC) website (http://www.modis.ornl.gov/modis/index.cfm). The first author was supported by the FS Chia Ph.D. scholarship and the Izaak Walton Killiam Memorial Scholarship of the University of Alberta, Canada.

## References


Boegh, E., H. Soegaard, H. Hanan, P. Kabat, and L. Lesch (1999), A remote sensing study of the NDVI-Ts relationship and the transpiration from sparse vegetation in the Sahel based on high-resolution data, *Remote Sens. Environ.*, *69*, 224–240, doi:10.1016/S0034-4257(99)00025-5.

Bounoua, L., G. J. Collatz, S. O. Los, P. J. Sellers, D. A. Dazilich, C. J. Tucker, and D. A. Randall (2000), Sensitivity of climate to changes in NDVI, *J. Clim.*, *13*, 2277–2292, doi:10.1175/1520-0442(2000)013<2277:SOCTCI>2.0.CO;2.

Ceccato, P., S. Flasse, S. Tarantola, S. Jacquemoud, and J. M. Gregoire (2001), Detecting vegetation leaf water content using reflectance in the optical domain, *Remote Sens. Environ.*, *77*, 22–33, doi:10.1016/S0034-4257(01)00191-2.

Ceccato, P., S. Flasse, and J. M. Gregoire (2002a), Designing a spectral index to estimate vegetation water content from remote sensing data: Part 2. Validation and applications, *Remote Sens. Environ.*, *82*, 198–207, doi:10.1016/S0034-4257(02)00036-6.

Ceccato, P., N. Gobron, S. Flasse, B. Pinty, and S. Tarantola (2002b), Designing a spectral index to estimate vegetation water content from remote sensing data: Part 1. Theoretical approach, *Remote Sens. Environ.*, *82*, 188–197, doi:10.1016/S0034-4257(02)00037-8.

Coops, N. C., R. H. Waring, and B. E. Law (2005), Assessing the past and future distribution and productivity of ponderosa pine in the Pacific Northwest using a process model, 3-PG, *Ecol. Modell.*, *183*, 107–124, doi:10.1016/j.ecolmodel.2004.08.002.

Curtis, P. S., P. J. Hanson, P. Bolstad, C. Barford, J. C. Randolph, H. P. Schimd, and K. B. Wilson (2002), Biometric and eddy-covariance based estimates of annual carbon storage in five eastern North American deciduous forests, *Agric. For. Meteorol.*, *113*, 3–19, doi:10.1016/S0168-1923(02)00099-0.

Danson, F. M., and P. Bowyer (2004), Estimating live fuel moisture content from remotely sensed reflectance, *Remote Sens. Environ.*, *92*, 309–321, doi:10.1016/j.rse.2004.03.017.

Desai, A. R., et al. (2008), Influence of vegetation and seasonal forcing on carbon dioxide fluxes across the upper midwest, USA: Implications for regional scaling, *Agric. For. Meteorol.*, *148*, 288–308, doi:10.1016/j.agrformet.2007.08.001.

Dirmeyer, P. A., and J. Shukla (1996), The effect on regional and global climate of expansion of the world's desert, *Q. J. R. Meteorol. Soc.*, *122*, 451–482, doi:10.1002/qj.49712253008.

Du, X., S. Wang, and Y. Zhou (2005), Monitoring and spatio-temporal evolution researching on vegetation leaf water in China, *IEEE Trans. Geosci. Remote Sens.*, *4*, 2365–2368.

Falge, E., et al. (2001), Gap filling strategies for long term energy flux data sets, *Agric. For. Meteorol.*, *107*, 71–77, doi:10.1016/S0168-1923(00)00235-5.

Gao, B. C. (1996), NDWI—A normalized difference water index for remote sensing of vegetation liquid water from space, *Remote Sens. Environ.*, *58*, 257–266, doi:10.1016/S0034-4257(96)00067-3.

Gebremichael, M., and E. P. Barros (2006), Evaluation of MODIS gross primary productivity (GPP) in tropical monsoon region, *Remote Sens. Environ.*, *100*, 150–166, doi:10.1016/j.rse.2005.10.009.

Ghulam, A., Q. Qin, and Z. Zhan (2007), Designing of the perpendicular drought index, *Environ. Geol.*, *52*, 1045–1052, doi:10.1007/s00254-006-0544-2.

Gilmanov, T. G., L. L. Tieszen, B. K. Wylie, L. B. Flanagan, A. B. Frank, M. R. Hafercamp, T. P. Meyers, and J. A. Morgan (2005), Integration of $CO_2$ and remotely sensed data for primary production and ecosystem respiration analyses in the northern Great Plains: Potential for quantitative spatial extrapolation, *Global Ecol. Biogeogr.*, *14*, 271–292, doi:10.1111/j.1466-822X.2005.00151.x.

Goulden, M. L., J. W. Munger, S. M. Fan, B. C. Daube, and S. C. Woofsy (1996), Measurements of carbon storage by long-term eddy correlation: Methods and a critical evaluation of accuracy, *Global Change Biol.*, *2*, 169–182, doi:10.1111/j.1365-2486.1996.tb00070.x.

Hashimoto, H., J. L. Dungan, M. A. White, F. Yang, A. R. Michaelis, S. W. Running, and R. R. Nemani (2008), Satellite-based estimation of surface vapor pressure deficits using MODIS land surface temperature data, *Remote Sens. Environ.*, *112*, 142–155, doi:10.1016/j.rse.2007.04.016.

Hazarika, M. K., Y. Yasuoka, A. Ito, and D. Dye (2005), Estimation of net primary productivity by integrating remote sensing data with an ecosystem model, *Remote Sens. Environ.*, *94*, 298–310, doi:10.1016/j.rse.2004.10.004.

Heinsch, F. A., et al. (2006), Evaluation of remote sensing based terrestrial production from MODIS using AmeriFlux eddy tower flux network observations, *IEEE Trans. Geosci. Remote Sens.*, *44*, 1908–1925, doi:10.1109/TGRS.2005.853936.

Huete, A. R. (2005), Global variability of terrestrial surface derived from MODIS visible to thermal-infrared channels, paper presented at International Geoscience and Remote Sensing Symposium, Inst. of Electr. and Electron. Eng., New York.

Hunt, E. R., Jr, and B. N. Rock (1989), Detection of changes in leaf water content using near-infrared and middle-infrared reflectances, *Remote Sens. Environ.*, *30*, 43–54, doi:10.1016/0034-4257(89)90046-1.

Ichii, K., Y. Matsui, K. Murakami, T. Mukai, Y. Yamguchi, and K. Ogawa (2003), A simple global carbon and energy coupled cycled model for global warming simulation: Sensitivity to the light saturation effect, *Tellus, Ser. B*, *55*, 676–691, doi:10.1034/j.1600-0889.2003.00035.x.

Intergovernmental Panel on Climate Change (2007), *Climate Change 2007: The Physical Science Basis, Contribution of Working Group 1 to the Fourth Assessment Report of the Intergovernmental Panel on Climate Change*, Cambridge Univ. Press, Cambridge, U. K.

Justice, D. H., et al. (1998), The Moderate Resolution Imaging Spectroradiometer (MODIS): Land remote sensing for global change research, *IEEE Trans. Geosci. Remote Sens.*, *36*(4), 1228–1249.

Karnieli, A., M. Bayasgalan, Y. Bayasgalan, N. Agam, S. Khudulmur, and C. J. Tucker (2006), Comments on the use of the vegetation health index over Mongolia, *Int. J. Remote Sens.*, *27*, 2017–2024, doi:10.1080/01431160500121727.

Kimball, J. S., M. A. White, and S. W. Running (1997), Biome BGC simulations of stand hydrologic processes for BOREAS, *J. Geophys. Res.*, *102*, 29,043–29,051, doi:10.1029/97JD02235.

Knorr, W., K. G. Schnitzler, and Y. Govaerts (2001), The role of bright desert regions in shaping North African climate, *Geophys. Res. Lett.*, *28*, 3489–3492, doi:10.1029/2001GL013283.

Landsberg, J. J., and R. H. Waring (1997), A generalized model of forest productivity using simplified concepts of radiation-use efficiency, carbon balance and partitioning, *For. Ecol. Manage.*, *95*, 209–228, doi:10.1016/S0378-1127(97)00026-1.

Lasdon, L. S., A. D. Waren, A. Jain, and M. Ratner (1978), Design and testing of a generalized reduced gradient code for nonlinear programming, *Trans. Math. Software*, *4*, 34–50, doi:10.1145/355769.355773.

Laval, K., and L. Picon (1986), Effect of change of the surface albedo on the Sahel climate, *J. Atmos. Sci.*, *43*, 2418–2429, doi:10.1175/1520-0469(1986)043<2418:EOACOT>2.0.CO;2.

Lucht, W., C. B. Schaaf, and A. H. Strahler (2000), An algorithm for the retrieval of albedo from space using semiempirical BRDF models, *IEEE Trans. Geosci. Remote Sens.*, *38*, 977–998, doi:10.1109/36.841980.

Makela, A., M. Pulkkinen, P. Kolari, F. Lagergren, P. A. Lindroth, D. Loustau, E. Nikinmaa, T. Vesala, and P. Hari (2008), Developing an empirical model of stand GPP with the LUE approach: Analysis of eddy covariance data at five contrasting coniferous sites in Europe, *Global Change Biol.*, *14*, 92–108.

Monteith, J. (1972), Solar radiation and productivity in tropical ecosystems, *J. Appl. Ecol.*, *9*, 747–766, doi:10.2307/2401901.

Ollinger, S. V., et al. (2008), Canopy nitrogen, carbon assimilation, and albedo in temperate and boreal forest: Functional relations and potential climate feedbacks, *Proc. Natl. Acad. Sci. U. S. A.*, *105*, 19,336–19,341, doi:10.1073/pnas.0810021105.

Potter, C. B., J. T. Randerson, C. B. Field, P. A. Matson, P. M. Vitousek, H. A. Mooney, and S. A. Klooster (1993), Terrestrial ecosystem production: A process model based on global satellite and surface data, *Global Biogeochem. Cycles*, *7*, 811–841, doi:10.1029/93GB02725.

Prince, S. D., and S. N. Goward (1995), Global primary production: A remote sensing approach, *J. Biogeogr.*, *22*, 815–835, doi:10.2307/2845983.

Rahman, A. F., D. A. Sims, V. D. Cordova, and B. Z. El-Masri (2005), Potential of MODIS EVI and surface temperature for directly estimating per-pixel ecosystem C fluxes, *Geophys. Res. Lett.*, *32*, L19404, doi:10.1029/2005GL024127.

Running, S. W., P. E. Thornton, R. Nemani, and J. M. Glassy (2000), Global terrestrial gross and net primary productivity from the earth observing system, in *Methods in Ecosystem Science*, edited by O. E. Sala, R. B. Jackson, and H. A. Mooney, pp. 44–57, Springer, New York.

Running, S. W., R. R. Nemani, F. A. Heinsch, M. Zhao, M. Reeves, and H. Hashimoto (2004), A continuous satellite-derived measure of global terrestrial primary production, *BioScience*, *54*, 547–560, doi:10.1641/0006-3568(2004)054[0547:ACSMOG]2.0.CO;2.

Schaaf, C. B., et al. (2002), First operational BRDF, albedo nadir reflectance products from MODIS, *Remote Sens. Environ.*, *83*, 135–148, doi:10.1016/S0034-4257(02)00091-3.

Schmid, H. P., H. B. Su, C. S. Vogel, and P. S. Curtis (2002), Footprint modeling for vegetation atmosphere exchange studies: A review and perspective, *Agric. For. Meteorol.*, *113*, 159–183, doi:10.1016/S0168-1923(02)00107-7.

Serrano, L., J. A. Gamon, and J. Penuelas (2000), Estimation of canopy photosynthetic and nonphotosynthetic components from spectral transmittance, *Ecology*, *81*, 3149–3162.

Sims, D. A., et al. (2006), On the use of MODIS EVI to assess gross primary productivity of North American ecosystems, *J. Geophys. Res.*, *111*, G04015, doi:10.1029/2006JG000162.

Sims, D. A., et al. (2008), A new model of gross primary productivity for North American ecosystems based solely on the enhanced vegetation index and land surface temperature from MODIS, *Remote Sens. Environ.*, *112*, 1633–1644, doi:10.1016/j.rse.2007.08.004.

Song, J. (1998), Diurnal asymmetry in surface albedo, *Agric. For. Meteorol.*, *92*, 181–189, doi:10.1016/S0168-1923(98)00095-1.

Spaulding, K. A. (1998), Neural metamorphic optimization algorithms, Masters thesis, Univ. of Texas at Austin, Austin.

Sun, D., and M. Kafatos (2007), Note on the NDVI-LST relationship and the use of temperature related drought indices over north America, *Geophys. Res. Lett.*, *34*, L24406, doi:10.1029/2007GL031485.

Turner, D. P., W. D. Ritts, W. B. Cohen, S. T. Gower, M. Zhao, S. W. Running, S. C. Wofsy, S. Urbanski, A. L. Dunn, and J. W. Munger (2003), Scaling gross primary production (GPP) over boreal and deciduous forest landscapes in support of MODIS GPP product validation, *Remote Sens. Environ.*, *88*, 256–270, doi:10.1016/j.rse.2003.06.005.

Turner, D. P., et al. (2005), Site-level evaluation of satellite-based global terrestrial GPP and NPP monitoring, *Global Change Biol.*, *11*(4), 666–684, doi:10.1111/j.1365-2486.2005.00936.x.

Urbanski, S., C. Barford, S. Wofsy, C. Kucharik, E. Pyle, J. Budney, K. McKain, D. Fitzjarrald, M. Czikowsky, and J. W. Munger (2007), Factors controlling $CO_2$ exchange on time scales from hourly to decadal at Harvard Forest, *J. Geophys. Res.*, *112*, G02020, doi:10.1029/2006JG000293.

Veroustraete, F., H. Sabbe, and H. Eerens (2002), Estimation of carbon mass fluxes over Europe using the C-Fix model and Euroflux data, *Remote Sens. Environ.*, *83*, 376–399, doi:10.1016/S0034-4257(02)00043-3.

Wan, Z., and J. Dozier (1996), A generalized split-window algorithm for retrieving land-surface temperature from space, *IEEE Trans. Geosci. Remote Sens.*, *34*, 892–905, doi:10.1109/36.508406.

Wang, S. (2005), Dynamics of surface albedo of a boreal forest and its simulation, *Ecol. Modell.*, *183*, 477–494, doi:10.1016/j.ecolmodel.2004.10.001.

Wang, S., and A. Davidson (2007), Impact of climate variations on surface albedo of a temperate grassland, *Agric. For. Meteorol.*, *142*, 133–142, doi:10.1016/j.agrformet.2006.03.027.

Wang, S., R. F. Grant, D. L. Verseghy, and T. A. Black (2001), Modelling plant carbon and nitrogen dynamics of a boreal aspen forest in CLASS—The Canadian Land Surface Scheme, *Ecol. Modell.*, *142*, 135–154, doi:10.1016/S0304-3800(01)00284-8.

Wang, S., R. F. Grant, D. L. Verseghy, and T. A. Black (2002a), Modelling carbon dynamics of boreal forest ecosystems using the Canadian Land Surface Scheme, *Clim. Change*, *55*, 451–477, doi:10.1023/A:1020780211008.

Wang, S., W. Chen, and J. Cihlar (2002b), New calculation methods of diurnal distributions of solar radiation and its interception by canopy over complex terrain, *Ecol. Modell.*, *155*, 191–204, doi:10.1016/S0304-3800(02)00122-9.

Waring, R. H., B. E. Law, M. L. Goulden, S. L. Bassow, R. W. McCreight, S. C. Wofsy, and F. A. Bazzaz (1995), Scaling gross ecosystem production at Harvard Forest with remote-sensing—A comparison of estimates from a constrained quantum-use efficiency model and Eddy-correlation, *Plant Cell Environ.*, *18*, 1201–1213, doi:10.1111/j.1365-3040.1995.tb00629.x.

Waring, R. H., N. C. Coops, W. Fan, and J. M. Nightingale (2006), MODIS Enhanced Vegetation Index predicts tree species richness across forested ecoregions in the contiguous U.S.A., *Remote Sens. Environ.*, *103*, 218–226, doi:10.1016/j.rse.2006.05.007.

Xiao, X. M., Q. Y. Zhang, B. Braswell, S. Urbanski, S. Boles, S. Wofsy, B. Moore, and D. Ojima (2004), Modeling gross primary production of temperate deciduous broadleaf forest using satellite images and climate data, *Remote Sens. Environ.*, *91*, 256–270, doi:10.1016/j.rse.2004.03.010.

Yuan, W., et al. (2007), Deriving a light use efficiency model from eddy covariance flux data for predicting daily gross primary production across biomes, *Agric. For. Meteorol.*, *143*, 189–207, doi:10.1016/j.agrformet.2006.12.001.

Zhao, M., F. A. Heinsch, R. R. Nemani, and S. W. Running (2005), Improvement of the MODIS terrestrial gross and net primary production global data set, *Remote Sens. Environ.*, *95*, 164–176, doi:10.1016/j.rse.2004.12.011.

T. Y. Gan and N. Jahan, Department of Civil and Environmental Engineering, University of Alberta, Edmonton, AB T6G 2W2, Canada. (tgan@ualberta.ca)